

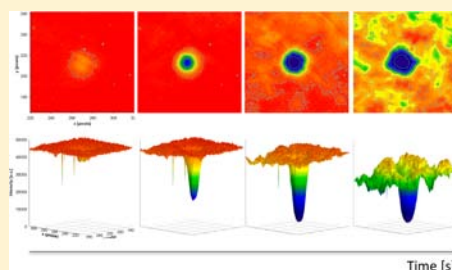
A Black Beam Borne by an Incandescent Field Self-Traps in a Photopolymerizing Medium

Kailash Kasala and Kalaichelvi Saravanamuttu*

Department of Chemistry and Chemical Biology, McMaster University, 1280 Main Street West, Hamilton, Ontario L8S 4M1, Canada

S Supporting Information

ABSTRACT: We report that a self-trapped black optical beam that is spatially and temporally incoherent forms spontaneously in a nascent photopolymerization system. The black beam inscribes a permanent cylindrical channel, which prevents the propagation of visible light even under passive conditions (in the absence of polymerization). The finding opens a powerful new mechanism to manipulate light signals from incoherent sources such as LEDs through selective suppression of light propagation. This contrasts with approaches employed by photonic crystals and optical waveguides, which concentrate and guide light intensity within spatially localized regions. The self-trapped black beam forms when a broad incandescent beam bearing a negligible depression was launched into a photopolymerizable medium. Because of refractive index changes caused by polymerization, the depression narrows, deepens, and continually rejects the visible spectrum of light until it stabilizes as a black beam that propagates over long distances (\gg effective Rayleigh range) without significant divergence. As refractive index changes due to polymerization are irreversible, the cylindrical region occupied by the self-trapped black beam is inscribed as a black channel waveguide in the medium.



1. INTRODUCTION

Self-trapped waves recur in stunning diversities and echelons of natural systems and are characterized by their ability to propagate without changing shape over unusually long distances in space or time. This nonlinear form of propagation, which can be described through variations of the nonlinear Schrödinger equation, governs critical processes in an extremely broad range of chemical, physical, and biological processes. A few examples are excitations along polymer chains,^{1,2} nonlinear chemical waves in reaction–diffusion systems,³ thermal solitons that drive biochemical cycles,⁴ localized vibrations along proteins,⁵ pulses along nerves⁶ and within the heart,⁷ sound,⁸ potentially catastrophic ocean waves,⁹ rolling clouds,¹⁰ and magnetosonic structures in space plasma.¹¹ Nonlinear waveforms are unified by mathematical expression and therefore, unsurprisingly, exhibit rich similarities in their internal dynamics and interactions.¹²

Self-trapped optical waves can be generated, probed, and made to interact under the precisely controlled conditions of an optics laboratory with beams or pulses of light. They are invaluable models of less tractable systems ranging from Bose Einstein condensates¹³ to rogue ocean waves.^{14,15} Self-trapped light beams can be elicited in a variety of photoresponsive materials such as photorefractive crystals, Kerr media, atomic vapor, and photopolymers, all of which undergo a change in refractive index upon exposure to an optical field.¹⁶ Positive index changes along the propagation path of the optical field counter the natural divergence of a beam (in space) or the dispersion of a pulse (in time). Under these nonlinear conditions, the beam or pulse can retain its spatial or temporal profile over long distances or time. Self-trapped beams were

generated only with laser light until 1997 when Mitchell and Segev reported self-trapping of light emitted by a tungsten filament.¹⁷ The polychromatic light emitted by such an incandescent source originates from the (poorly correlated) relaxation of excited electronic states and, as a result, has extremely weak correlations of phase and amplitude over space and in time. For example, the divergence and familiar diffusivity of sunlight is exceptionally large (as compared, for example, to a Gaussian laser beam) and is a direct consequence of its spatial and temporal incoherence. Under certain conditions in a photorefractive crystal, incandescent light was found to spatially self-trap and propagate without diverging over long distances (\gg effective Rayleigh range).¹⁷ The discovery of spatially self-trapped incandescent light was seminal to the field because it broke more than three decades of assumption that nonlinear propagation was the exclusive behavior of coherent light fields.¹⁷ The finding has stimulated new inquiry and challenged established knowledge of spatial correlation,¹⁸ shape,¹⁹ frequency distribution,²⁰ and modulation instability (MI)²¹ associated with the nonlinear propagation of light beams. Importantly, self-trapped incoherent beams promise greater fidelity to localized wavepackets in natural systems, which, subject to inherent thermal or quantum fluctuations, must be composed of waves that are weakly correlated in space and time.²²

Self-trapped dark incoherent beams are a particularly intriguing species, which comprise a nondivergent core of reduced intensity embedded in a bright, incoherent background

Received: June 11, 2012

Published: July 25, 2012

beam. Discovered and studied predominantly in photorefractive crystals, self-trapped dark incoherent beams emerge under self-defocusing conditions where index changes induced in the dark regions of a nonuniform optical field exceed those induced in the bright regions.^{23–25} When a bright background beam bearing an amplitude depression (dark core) is launched into a self-defocusing medium, light intensity from the background defocuses and leaks into the higher-index dark core. This effectively suppresses the natural divergence of the dark core, which consequently propagates as a self-trapped beam. Because they necessarily contain background light, dark beams generated in photorefractive crystals are characteristically gray (i.e., contain a significant amount of light intensity).²³

We report the discovery of a new incoherent species, a self-trapped black beam embedded in an incandescent field, which emerges in a nascent photopolymerizable medium. The black beam differs fundamentally from previous examples of dark incoherent beams: it evolves under the self-focusing conditions generated by photopolymerization and amplifies by continually dispelling light intensity to its surroundings until it is rendered entirely black. Remarkably, this to our knowledge is the first example of the spontaneous and complete extinction of light intensity in a spatially and temporally incoherent field. (Self-trapped black beams could until now only be achieved with coherent optical fields.²⁶) By imaging the distribution of light intensity in the medium and monitoring its evolution, we gain an understanding of the mechanism underlying this seemingly counterintuitive discovery.

2. RESULTS AND DISCUSSION

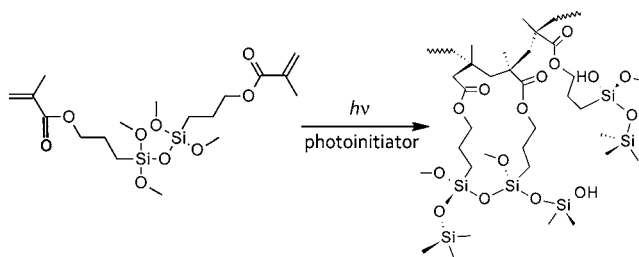
We found that a weak, noise-like depression (dip) in a uniform beam of incoherent white incandescent light spontaneously narrowed, deepened, and transformed into a self-trapped black beam as it propagated in a photopolymerizable organosiloxane gel (see MOVIE_S1, Experimental in the Supporting Information). Under linear conditions (in the absence of polymerization), the dip was negligible noise that rapidly disappeared with propagation distance due to the characteristically large divergence²⁷ of the background white light. By contrast, when the dip-embedded beam initiated free-radical polymerization as it propagated through the medium, the system was pushed off-equilibrium into a nonlinear regime. Under these conditions, the dip amplified into a dark beam, which spontaneously rejected light until it transformed into a self-trapped black beam. Because it was embedded in an optical field that was spatially and temporally incoherent, the black beam was extremely poorly correlated in phase and amplitude in space and time. The self-trapped black beam permanently inscribed a channel in the photopolymer, which rejected white light even under linear conditions.

2.1. A Suitable Medium for the Nonlinear Propagation of Incoherent White Light. Incoherent beams self-trap under very specific conditions:¹⁷ unlike coherent laser radiation, incandescence from the sun or the tungsten filament that we employ suffers random variations in phase and amplitude, typically at the femtosecond time scale. A white light beam from an incandescent source can be considered an ensemble of rapidly fluctuating intensity speckles. This chaotic,²⁸ spatially, and temporally incoherent wavepacket can self-trap in a medium that undergoes a photoinduced index change over an interval that greatly exceeds the femtosecond regime.¹⁷ Such a noninstantaneous system, like the human eye, for example, responds to the time-averaged (smoothed) intensity profile of a

white light beam and is unperturbed by the phase and amplitude fluctuations that would otherwise inhibit self-trapping.²⁹ The photoinduced index change must moreover saturate over time and be sufficiently large to self-consistently guide the multiple optical modes that constitute white light.¹⁶ Should these prerequisites be satisfied, then an incoherent beam self-traps as a whole, conserving energy and spectral composition.^{30,31}

On the basis of our previous findings that self-trapping³⁰ and other forms of nonlinear propagation of bright incoherent light^{32–34} can be elicited through photoinitiated free-radical polymerization, we intuited that the same chemical process could also host dark incoherent beams. The organosiloxane photopolymer selected for the dark beam experiments satisfies the requirement of a noninstantaneous, saturable, and large photoresponse:³⁰ when exposed to white light in the presence of a photoinitiator, methacrylate substituents of the organosiloxane undergo free-radical polymerization (Scheme 1), which produces a local increase in refractive index (Δn).

Scheme 1. Photoinitiated Free-Radical Polymerization of Organosiloxane Photopolymer



The time scale of Δn changes, which is determined by the polymerization rate, varies from seconds to minutes over the course of the reaction. This translates into a photoresponse time that is at least 13 orders of magnitude greater than the femtosecond fluctuations of incandescent light. As polymerizable moieties are depleted in the medium, the index change of the organosiloxane reaches a maximum value of ~ 0.006 ,³⁵ which is sufficient to support all of the modes of white light.³⁰

2.2. Experimental Evidence of Self-Trapped Black Beam. To generate the incoherent self-trapped dark beam, we passed a broad, collimated beam of white light emitted by a quartz-tungsten-halogen lamp through an amplitude mask, which introduced a weak, circular depression in the optical field (see Experimental, Supporting Information). The dip-containing beam was focused onto the entrance face of a transparent cuvette containing the organosiloxane photopolymer, which was sensitized to visible wavelengths with a titanocene photoinitiator. At the entrance face of the sample, the dip had a width ($1/e^2$) of $124 \mu\text{m}$, while the background beam was $5317 \mu\text{m}$ wide and therefore considered to extend infinitely in the vicinity of the dip (henceforth referred to as the infinite background beam). The dip, with a relative intensity of 66%, was slightly weaker in intensity than the background beam, which had an intensity of 77%. The dip broadened and increased in intensity as it propagated through the medium under linear conditions. This is a consequence of the inherently large divergence of the incoherent background beam.²⁷ After a propagation distance (z) of 6.0 mm, the dip was extremely faint with a diameter of approximately $400 \mu\text{m}$ and a relative intensity of 67%, making it nearly indistinguishable from the

background beam, which had decreased in intensity to 72%. To study the effect of free-radical polymerization on the propagation dynamics of the dip and its consequent transformation into a self-trapped black beam, we monitored the spatial intensity profile of the dip-embedded beam at a propagation distance (z) of 6.0 mm with a CCD camera.

Typical experimental results are shown as temporal plots of width and intensity of the dip at $z = 6.0$ mm (Figure 1a).

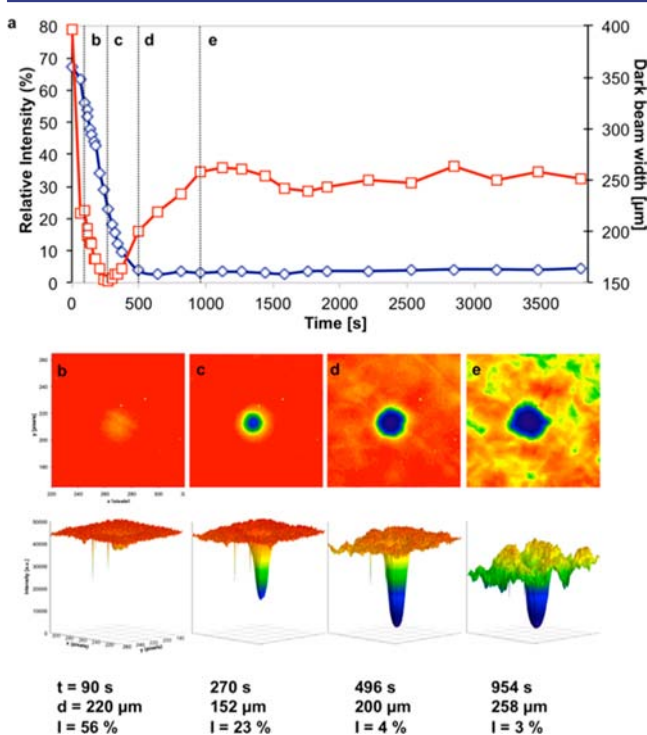


Figure 1. Formation and evolution of self-trapped black beam due to photoinitiated free-radical polymerization in the organosiloxane observed through (a) temporal plots of relative intensity (\diamond) and width (\square) at $z = 6.0$ mm. Dotted lines correspond to 2-D and 3-D spatial intensity profiles of the black beam acquired at $z = 6.0$ mm at (b) 90 s, (c) 270 s, (d) 496 s, and (e) 954 s at $z = 6$ mm. The black beam width (fwhm) and relative intensity at each time are indicated. The scales in (b) apply to (c,d). (See movie in the Supporting Information (Movie_S1).)

Corresponding spatial profiles (Figure 1b–e) and a movie (MOVIE_S1, Supporting Information) are also presented. The dip underwent a sequence of striking changes when polymerization was initiated along the propagation path of the beam: within 90 s, the dip became visible at $z = 6.0$ mm, narrowing by almost one-half from 400 to 220 μm and darkening from a relative intensity of 67% to 56%. Over the next 180 s, the dip darkened to 23% and reached a minimum width of 152 μm , which was comparable to its width of 124 μm at $z = 0.0$ mm. This signified the transformation of the dip into a self-trapped dark beam, which traveled through the medium without significant broadening. In the next 200 s, the self-trapped dark beam widened to 200 μm but continued to reject light until its relative intensity decreased to an average value of 4%. This value, being indistinguishable from the dark noise (3%) of the CCD detector, meant that the self-trapped beam was now effectively black. The self-trapped black beam widened to 250 μm over the next 460 s but remained stable at this width

without reverting to its original divergent form (400 μm) and remained black for as long as it was monitored (~ 4000 s).

The self-trapped black beam inscribed a permanent cylindrical channel from the entrance to the exit face of the photopolymer. Optical microscopy revealed the 150 μm -wide structure, which appeared black in an otherwise uniformly polymerized bright medium (Figure 2a). Remarkably, this

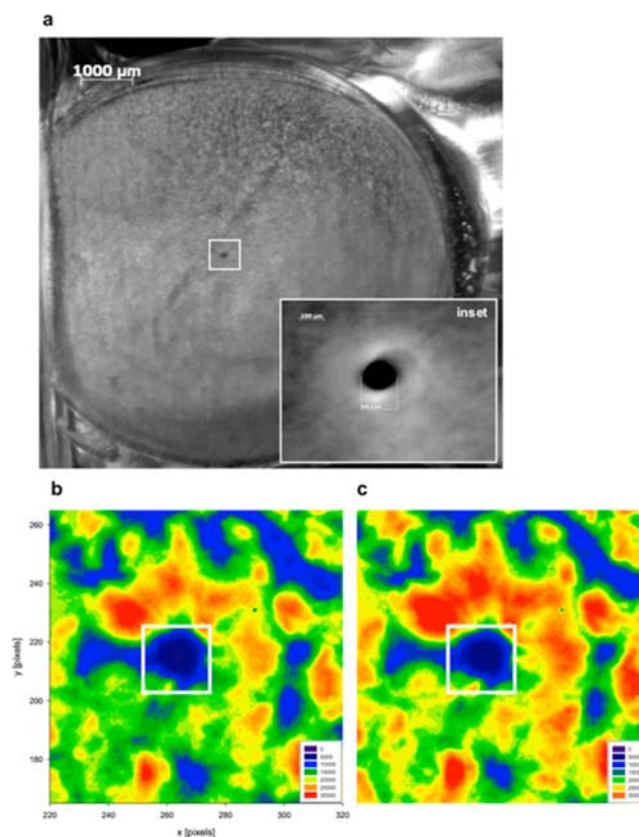


Figure 2. (a) Optical micrograph of self-induced black channel in the organosiloxane. The 150 μm -wide channel (inset) is embedded in an otherwise uniformly photopolymerized area, which corresponds to the background beam. Comparison of the spatial intensity profiles at $z = 6.0$ mm of the (b) self-trapped dark beam at $t = 3798$ s and a broad white light beam launched into the (c) corresponding self-inscribed channel show negligible differences: the relative intensities (widths) of the self-trapped black beam (b) and channel (c) were 4.5% (251 μm) and 5% (235 μm), respectively. For clarity, the (b) black beam and (c) black channel are enclosed by a white square. Intensity variations across the background beam in (b) and (c) are due to modulation instability of the background beam, which emerges at late times in the experiment.

channel was black and was impenetrable to white light even under linear conditions. To quantify its exclusion of light, a broad and entirely uniform white light beam was launched into the sample and monitored at $z = 6.0$ mm. The beam propagated in all regions of the sample but was selectively excluded from the black channel. The relative intensity transmitted through the channel was 5%, which was nearly indistinguishable from the dark noise (3%) of the CCD camera (Figure 2c).

2.3. Proposed Mechanism of Self-Trapped Black Beam Formation. The origin and evolution of the self-trapped black beam is understood by considering the refractive index changes induced along the path of the dip-embedded

background beam. Index changes due to photoinitiated free-radical polymerization in the organosiloxane vary in space and time according to:³⁶

$$\Delta n(r, z, t) = \Delta n_s \left\{ 1 - \exp \left[-\frac{1}{U_0} \int_0^{t-\tau} |E(t)|^2 dt \right] \right\} \quad (1)$$

where Δn_s is the maximum index change (at saturation), U_0 is the critical energy required to initiate polymerization, τ is the monomer radical lifetime (assumed to be negligible), and $E(t)$ is the electric field amplitude of the optical field. Equation 1 must be combined with the general expression for beam propagation in a photoresponsive medium, which is given by the nonlinear paraxial wave equation:³⁷

$$ik_0 n_0 \frac{\partial \mathcal{E}}{\partial z} + \frac{1}{2} \nabla_t^2 \mathcal{E} + k_0^2 n_0 \Delta n \mathcal{E} + \frac{i}{2} k_0 n_0 \alpha \mathcal{E} = 0 \quad (2)$$

where α is the attenuation coefficient of the medium at wavelength λ corresponding to the free space wavenumber, $k_0 = \omega/c$. Equation 2 describes the reciprocal interactions between a beam and self-induced refractive index changes along its propagation path. Solutions of eq 2 show that the natural divergence of a beam in the directions orthogonal to its propagation path (represented by the transverse Laplacian term) is suppressed by self-induced refractive index changes (Δn) along its propagation path. This positive nonlinearity (self-focusing conditions), as extensively demonstrated by theory and experiment,^{37,38} enables self-trapping of bright beams. Below, we propose why the same positive nonlinearity can elicit the converse species, a self-trapped black beam.

We propose and then prove through additional experiments that the self-trapped black beam forms through the following sequence of events: the dip introduces a weak inhomogeneity in the otherwise uniform rate of polymerization and consequent Δn induced by the background beam. According to eq 1, Δn induced by the background beam at early times marginally exceeds that induced by the dip. Because light preferentially propagates in regions of even weakly elevated index,^{23,25} the dip-induced perturbation in refractive index triggers the efflux of intensity from the dip to the background. As light concentrates in the regions of the background beam, the local refractive index increases further, causing additional outflow of intensity from the dip. Continually depleted in this way, the dip turns black as the background intensity reaches maximum. Simultaneously, Δn of the background becomes sufficiently strong to effect self-trapping of the background beam through the nonlinear process described by eq 2. The self-trapped and therefore nondivergent background beam in turn suppresses the broadening of the embedded dip by “holding” it in focus along the propagation path. During this process, the background continually increases in refractive index and withdraws intensity from the dip. Once polymerizable methacrylate units in the background are depleted and Δn saturates, the system equilibrates, and both background and self-trapped black beams become stable.

The emergence of the black beam relies on the strong gradient in refractive index between the black and bright regions of the optical field. The refractive index gradient in turn originates from strong variations in the extent of free-radical polymerization in the originally isotropic medium; the rate of polymerization maximizes in the most intense, bright background regions and minimizes in the dark regions of the evolving self-trapped beam. Because Δn is proportional to the

extent of polymerization in the medium, the stable self-trapped black beam occupies the least polymerized region.

2.4. Experimental Verification of Mechanism. To prove the proposed mechanism, we repeated the experiment by replacing the infinite background beam with one of smaller width (henceforth, the finite background beam). This enabled quantitative correlation of the spatial intensity profiles of the background and dip.³⁹ Because its width (1146 μm) exceeded that of the dip (125 μm) by an order of magnitude, the background beam could still be considered uniform in the dip’s vicinity.

First, we confirmed that a self-trapped dark beam could be generated with this new configuration and that it followed dynamics similar to that with the infinite beam (Figure 3).

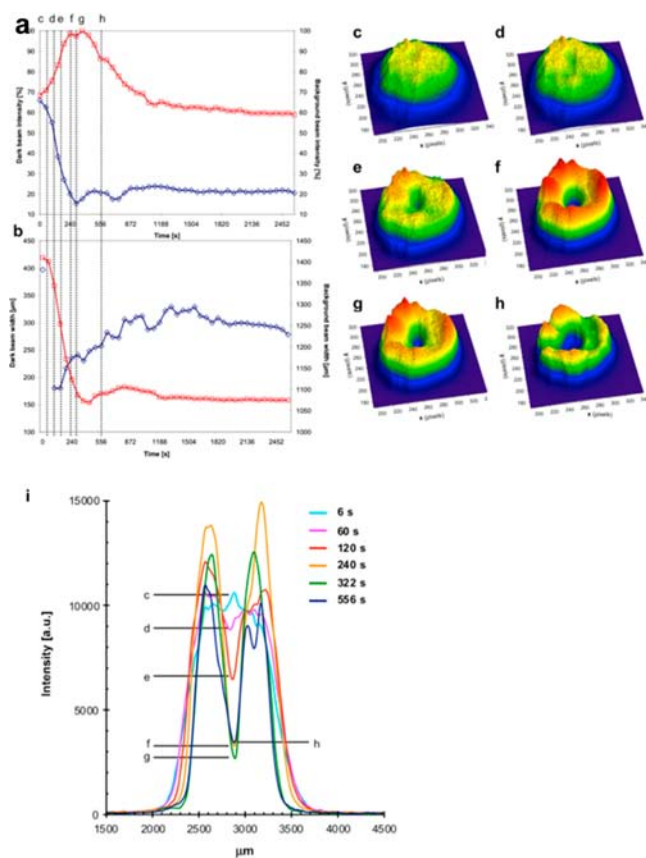


Figure 3. Formation and evolution of self-trapped dark incoherent beam in a background beam of finite width (1146 μm) observed through temporal plots of (a) relative intensities and (b) widths of the dark beam (\diamond) and background beam (\square) at $z = 6.0$ mm. Dotted lines correspond to spatial profiles of the beam acquired at $z = 6.0$ mm at (c) 6 s, (d) 60 s, (e) 120 s, (f) 240 s, (g) 322 s, and (h) 556 s. Corresponding 1-D profiles in (i) trace the deepening and slight widening of the self-trapped dark beam over time.

Then, we compared temporal plots of widths (Figure 3a) and intensities (Figure 3b) of the background and the dip at $z = 6.0$ mm to test the validity of the proposed mechanism. Experimental results were in excellent agreement with the proposed mechanism: within 120 s, the predicted self-trapping of the background beam was detected by its decrease in width from 1400 to 1343 μm and increase in relative intensity from 68% to 76%. Self-trapping of the background suppressed the divergence and caused simultaneous self-trapping of the dip, which narrowed substantially (from 400 to 180 μm) with a

Table 1. Experimental Parameters of Self-Trapped Black and Dark Beams in the Organosiloxane Photopolymers

background beam width at $z = 6 \text{ mm}$ [μm]	time of dark beam self-trapping [s]	minimum dark beam width [μm]	corresponding background beam width [μm]	minimum dark beam intensity [%]	final dark beam width [μm]	final bright beam width [μm]
5351	270	152	n/a	3	251	n/a
1410	120	180	1254	21	279	1075
848	120	102	662	31	118	515

concurrent decrease in relative intensity (66% to 55%). Once self-trapped, the dark beam widened to $217 \mu\text{m}$ at 180 s (the same trend was observed with the infinite background in Figure 2). During the same time, the background beam narrowed further to $1171 \mu\text{m}$. The cause of dark beam-widening is evident in the sequence of 1-D spatial profiles (Figure 3i). At early times, narrowing of the background beam was sufficient to almost exactly counter the natural divergence of the embedded dip. However, as its local Δn continued to rise, the background beam began to self-focus. While the outer diameter of the background beam decreased, its inner boundaries were drawn away from the center, effectively widening the dark beam. Although it widens slightly after reaching a minimum width, the dark beam remains self-trapped and is significantly narrower as compared to its original width.

In the proposed mechanism, dark beam formation is governed by the outflow of intensity from the dip to the background. Accordingly, we observed a precise reciprocity in intensity transfer between the dip and background beam (Figure 3a): the rate of increase of background intensity exactly matched the rate of decrease of dip intensity; the background and dip intensities maximized and minimized, respectively, at $\sim 322 \text{ s}$. At long times ($\sim 1200 \text{ s}$), as the rate of polymerization and refractive index changes became negligible, the system reached equilibrium, and light transfer from the dark to the bright regions ceased. The dark beam stabilized with an average width of $305 \mu\text{m}$, remained dark (relative intensity of $\sim 21\%$), and did not revert to its original divergent form for as long as it was monitored ($\sim 3500 \text{ s}$).

Although the self-trapped dark beam generated with the finite background beam became significantly dark (relative intensity of $\sim 21\%$), it did not turn completely black. In fact, we repeated the experiment with an even smaller background beam ($614 \mu\text{m}$) and found that, although a self-trapped dark beam formed (Figure S2, Supporting Information), its minimum intensity was 31% (Table 1). For the infinite background beam, the dip is the only region of depressed intensity in an otherwise uniform field. It is therefore the only source from which intensity is withdrawn during self-focusing of the background beam and is ultimately rendered black. A smaller background beam can withdraw intensity from the dip as well as the regions surrounding its outer boundary (these regions initially contain intensity due to the divergence of the background beam with propagation distance). Refractive index changes in the background therefore saturate, and the system reaches equilibrium before the intensity of the dip is entirely depleted. This accounts for the residual intensity in the self-trapped dark beam in the case of the finite and small background beams. Self-trapping parameters for the three different background beams are presented for comparison in Table 1. Self-trapping of the dip, which was observed in all cases, followed the same dynamics, initially decreasing to a minimum width and showing a slight increase as the background beam continued to self-focus.

2.5. Comparison with Self-Trapped Incoherent Dark Beams in Photorefractive Crystals. The self-trapped black and dark beams generated in the organosiloxane differ fundamentally from the only other known self-trapped dark incoherent beams, which form in photorefractive crystals through the electro-optic effect.²³ These studies have predominantly employed partially spatially incoherent, quasi-monochromatic laser light, although the interactions between a pair of self-trapped spatially and temporally incoherent dark beams have been examined.²⁵ Self-trapped dark beams in appropriately biased photorefractive crystals emerge from a negative nonlinearity (self-defocusing conditions): in contrast to the photopolymer system, the greatest changes in refractive index are induced by the dip embedded in a background beam. The inner boundaries of the background beam therefore expand as they gravitate into the higher-index dark region. This self-defocusing of the background beam compensates for the divergence of the dark beam, enabling it to self-trap. Incoherent dark beams formed in this way necessarily contain light intensity and thus are always gray, that is, contain more light intensity than the dip at the input face of the crystal. Until the current report, it was assumed that self-trapped black beams could only be generated with coherent laser beams.

3. SUMMARY AND OUTLOOK

We found that photopolymerization provides an accessible route to self-trapped dark beams including black beams that are spatially and temporally incoherent. These fundamentally new optical species form because of the specific way in which refractive index changes due to polymerization evolve over space and in time. Our findings bring together research into the nonlinear propagation of both chemical and optical waves. Although traditionally disparate research areas, both share the objective of gaining insight into the dynamics of nonlinear waves: we propose that a self-trapped beam is in fact a spatially localized reaction field that exhibits nonlinear propagation. While nonlinear chemical waves can be excited in reaction–diffusion systems,^{3,40} the nonlinear propagation of polymerization waves in our system is established through the reciprocal interactions between a light beam and a photochemical medium. By deliberately modifying the spatial profile of the optical field, that is, by introducing a dip, it is possible to precisely control the spatial and temporal evolution of the reaction field. Because light is a participant in the reaction, optical imaging provides sensitive insight into the kinetics and 3-D spatial evolution of the reaction field that would otherwise be impossible to acquire.

The random phase structure of the black beam embedded in the incandescent field is an intriguing optical paradox, as until now, self-trapped black beams necessarily had precisely defined phase structure.²⁶ Staging collisions between self-trapped incoherent black beams themselves and with bright/dark and incoherent/coherent beams could provide insight into their phase structure and also open possibilities to deliberately

change the coherence of colliding beams, which would be extremely important in designing active photonic devices.¹⁶

Channels induced by self-trapped dark beams typically possess greater indices of refraction relative to their surroundings and therefore behave as conventional waveguides that confine and guide light.²⁴ By contrast, the channels induced by self-trapped black beams in our system suppress the transmission of visible light over long distances (\gg effective Rayleigh range). This is particularly important as dark features in incoherent beams (like shadows cast by daylight) suffer significant blurring and become gray after very short propagation distances. The self-induced black channels open a powerful alternate mechanism to control the flow of light through selectively suppressing light transmission over long distances. We have previously shown that three types of interactions, fusion, fission, and repulsion, take place between a pair of self-trapped incoherent bright beams.³⁴ Similar interactions between self-trapped dark beams would provide a means to induce complex black waveguide structures. These mechanisms could be applied to light from inexpensive and miniaturized incoherent sources such as LEDs, which are critical in the development of microphotonics and integrated-optics devices. We have already carried out numerical simulations that provide theoretical proof of the concept that self-trapped black beams form during polymerization (Supporting Information); these will be extended in the future to spatially and temporally incoherent and polychromatic optical fields to model the experimental findings described in this Article.

■ ASSOCIATED CONTENT

📄 Supporting Information

(1) A movie of the emergence of the self-trapped black beam: temporal evolution of 2-D and 3-D spatial intensity profiles of a dip-embedded incandescent beam acquired at a path length of 6.00 mm in the photopolymerizable organosiloxane. (2) Document containing (i) experimental section, (ii) temporal plots tracing effect of background beam diameter on the dynamics of a self-trapping black beam, and (iii) simulations of the self-trapping of dark beams (in a coherent field) in a photopolymer. This material is available free of charge via the Internet at <http://pubs.acs.org>.

■ AUTHOR INFORMATION

Corresponding Author

kalai@mcmaster.ca

Notes

The authors declare no competing financial interest.

■ ACKNOWLEDGMENTS

Funding from the Natural Sciences and Engineering Research Council, Canadian Foundation for Innovation, Ontario Institute of Technology, and McMaster University is gratefully acknowledged. We thank CIBA GEIGY, Canada, for generous donation of the photoinitiator IRGACURE-784.

■ REFERENCES

- (1) Su, W. P.; Schrieffer, J. R. *Proc. Natl. Acad. Sci. U.S.A.* **1980**, *77*, 5626–5629.
- (2) Tretiak, S.; Saxena, A.; Martin, R. L.; Bishop, A. R. *Proc. Natl. Acad. Sci. U.S.A.* **2003**, *100*, 2185–2190.
- (3) Tuckwell, H. C. *Science* **1979**, *205*, 493–495.

- (4) Careri, G.; Wyman, J. *Proc. Natl. Acad. Sci. U.S.A.* **1984**, *81*, 4386–4388.
- (5) Davydov, A. S. *J. Theor. Biol.* **1979**, *66*, 379–387.
- (6) Heimbürg, T.; Jackson, A. D. *Proc. Natl. Acad. Sci. U.S.A.* **2005**, *102*, 9790–9795.
- (7) Aslanidi, O. V.; Mornev, O. A. *J. Biol. Phys.* **1999**, *25*, 149–164.
- (8) Spadoni, A.; Daraio, C. *Proc. Natl. Acad. Sci. U.S.A.* **2010**, *107*, 7230–7234.
- (9) Witman, J. D.; Leichter, J. J.; Genovese, S. J.; Brooks, D. A. *Proc. Natl. Acad. Sci. U.S.A.* **1993**, *90*, 1686–1690.
- (10) Porter, A.; Smyth, N. F. *J. Fluid Mech.* **2002**, *454*, 1–20.
- (11) Pokhotelov, O. A.; Onishchenko, O. G.; Balikhin, M. A.; Stenflo, L.; Shukla, P. K. *J. Plasma Phys.* **2007**, *73*, 981–992.
- (12) Infeld, E.; Rowlands, G. *Nonlinear Waves, Solitons and Chaos*; Cambridge University Press: New York, 1990.
- (13) Proukakakis, N. P.; Parker, N. G.; Frantzeskakis, D. J.; Adams, C. S. *J. Opt. B: Quantum Semiclassical Opt.* **2003**, *6*, S380–S391.
- (14) Solli, D. R.; Ropers, C.; Koonath, P.; Jalali, B. *Nature* **2007**, *450*, 1054–1057.
- (15) Kibler, B.; Fatome, J.; Finot, C.; Millot, G.; Dias, F.; Genty, G.; Akhmediev, N.; Dudley, J. M. *Nat. Phys.* **2010**, *6*, 790–795.
- (16) *Spatial Solitons*; Trillo, S., Torruellas, W., Eds.; Springer: New York, 2001.
- (17) Mitchell, M.; Segev, M. *Nature* **1997**, *387*, 880–883.
- (18) Buljan, H.; Šiber, A.; Soljačić, M.; Segev, M. *Phys. Rev. E* **2002**, *66*, 035601.
- (19) Buljan, H.; Šiber, A.; Soljačić, M.; Schwartz, T.; Segev, M.; Christodoulides, D. N. *Phys. Rev. E* **2003**, *68*, 036607.
- (20) Buljan, H.; Segev, M.; Soljačić, M.; Efremidis, N. K.; Christodoulides, D. N. *Opt. Lett.* **2003**, *28*, 1239.
- (21) Schwartz, T.; Carmon, T.; Buljan, H.; Segev, M. *Phys. Rev. Lett.* **2004**, *93*, 223901.
- (22) Cohen, O.; Bartal, G.; Buljan, H.; Carmon, T.; Fleischer, J. W.; Segev, M.; Christodoulides, D. N. *Nature* **2005**, *433*, 500–503.
- (23) Tamer, H.; Coskun, T. H.; Christodoulides, D. N.; Mitchell, M.; Chen, Z.; Segev, M. *Opt. Lett.* **1998**, *23*, 418–420.
- (24) Chen, Z.; Mitchell, M.; Segev, M.; Coskun, T. M.; Christodoulides, D. N. *Science* **1998**, *280*, 889–892.
- (25) Liu, Z.-H.; Liu, S.-M.; Guo, R.; Gao, Y.-M.; Song, T.; Zhu, N.; Qu, D. *Chin. Phys. Lett.* **2007**, *24*, 446–449.
- (26) Kivshar, Y. S.; Luther-Davies, B. *Phys. Rep.* **1998**, *298*, 81–197.
- (27) Born, M.; Wolf, E. *Principles of Optics, Electromagnetic Theory of Propagation, Interference and Diffraction of Light*, 7th ed.; Cambridge University Press: UK, 2002; Chapter 7.
- (28) Li, Y.; Krinsky, S.; Lewellen, J. W.; Kim, K.-J.; Sajaev, V.; Milton, S. V. *Phys. Rev. Lett.* **2003**, *91*, 243602–243605.
- (29) Incoherent spatial solitons have more recently been generated in media with an instantaneous but nonlocal response: Rotschild, C.; Schwartz, T.; Cohen, O.; Segev, M. *Nat. Photonics* **2008**, *2*, 371–376.
- (30) Zhang, J.; Kasala, K.; Rewari, A.; Saravanamuttu, K. *J. Am. Chem. Soc.* **2006**, *128*, 406–407.
- (31) Zhang, J.; Saravanamuttu, K. *J. Am. Chem. Soc.* **2006**, *128*, 14913–14923.
- (32) Burgess, I. B.; Shimmell, W. E.; Saravanamuttu, K. *J. Am. Chem. Soc.* **2007**, *129*, 4738–4746.
- (33) Burgess, I. B.; Ponte, M. R.; Saravanamuttu, K. *J. Mater. Chem.* **2008**, *18*, 4133–4139.
- (34) Kasala, K.; Saravanamuttu, K. *Appl. Phys. Lett.* **2008**, *93*, 051111–051111-3.
- (35) Saravanamuttu, K.; Du, X. M.; Najafi, S. I.; Andrews, M. P. *Can. J. Chem.* **1998**, *76*, 1717–1729.
- (36) Kewitsch, A.; Yariv, A. *Opt. Lett.* **1996**, *21*, 24–26.
- (37) Monro, T. M.; De Sterke, C. M.; Poladian, L. *J. Mod. Opt.* **2001**, *48*, 191–238.
- (38) Villafranca, A. B.; Saravanamuttu, K. *J. Phys. Chem. C* **2008**, *112*, 17388–17396.
- (39) This was not possible in the case of the infinite beam, which was too broad to be accurately imaged in its entirety by the CCD.
- (40) Vanag, V. K.; Epstein, I. R. *Science* **2001**, *294*, 835–837.